

Supplementary Materials to

“The Mediterranean Rhodes Gyre: modelled impacts of climate change, acidification and fishing”

by Sonja M. van Leeuwen, Jonathan A. Beecham, Luz M. García-García, Robert Thorpe

Section S1. Coupled model setup

S1.1 Temperature and salinity profiles

CTD data from ICES (<https://ocean.ices.dk/HydChem>) was used to construct temperature and salinity profiles. From this data smoothed, monthly profiles were constructed that mimicked the observational data and depended on the local air temperature, to ensure profiles could adapt to future climatic conditions. Evaporation was also included in the model, allowing for salinity changes in the surface layer that can lead to overturning. S profiles were relaxed to by 20 days in all layers. T profiles relaxation periods were 20 days (middle, bottom layers) and 1 day (surface layers).

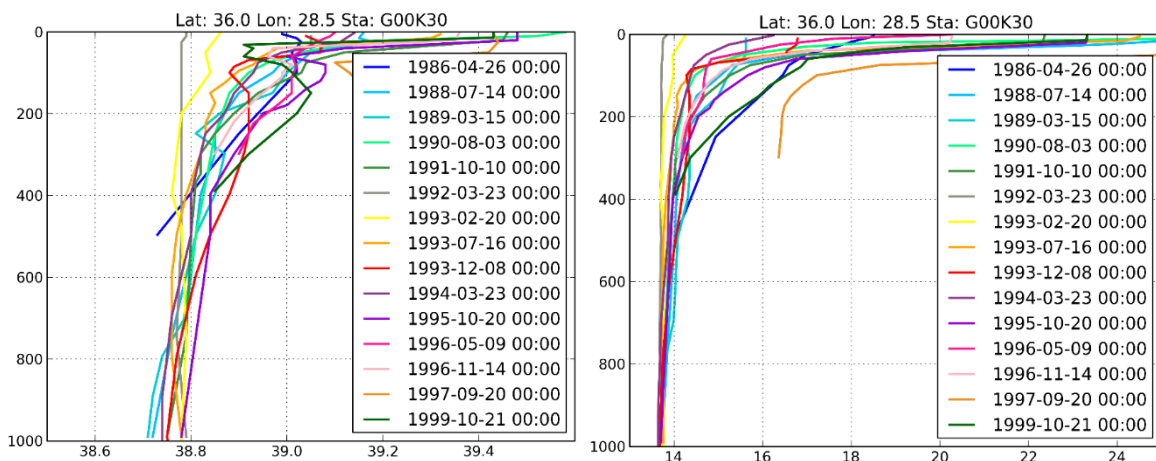


Figure S1: CTD profiles used in simulating the vertical structure of the Rhodes gyre center. Left: salinity profiles and right: temperature profiles. Vertical axis displays

S1.2 Atmospheric deposition

Atmospheric deposition values were estimated from Zhang et al. (2015). Dust deposition in the Mediterranean was estimated as $15 \text{ g m}^{-3} \text{ y}^{-1}$ (their Figure 12b), and percentage within dust (their Table 4) for the Mediterranean was applied, resulting in the following atmospheric deposition values presented in Table S1. Note that nitrogen estimates are not provided in Zhang et al. (2015), hence the Redfield ratio was applied (16 N : 1 P) to the phosphorous value.

Table S1: Applied atmospheric deposition values. The N contribution was based on the P contribution and assuming the Redfield ratio.

Compound	Percentage within dust	Atmospheric deposition
N		0.0176 mmol N/m ² /d
P	0.08 %	0.0011 mmol P /m ² /d
Si	29.14 %	0.4262 mmol Si/m ² /d
Fe	2.9 %	21.3409 $\mu\text{mol Fe /m}^2/\text{d}$

Section S2. Future climatic conditions

The applied future climate and ocean acidification scenarios follow the RCP4.5 and RCP8.5 carbon emissions pathways. Here Figure S2 shows the associated atmospheric pCO₂ levels for these scenarios, while Figure S3 visualizes the meteorological changes for the 2 pathways up to the year 2100, according to the CMIP5 projection.

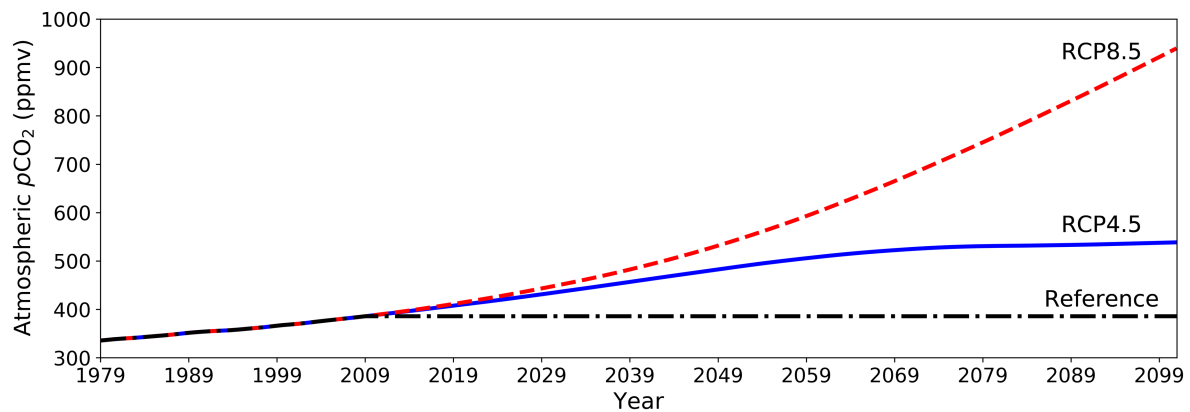


Figure S2: the applied atmospheric pCO₂ levels for each climate change scenario. The reference state assumed no increase in atmospheric pCO₂ after 2008.

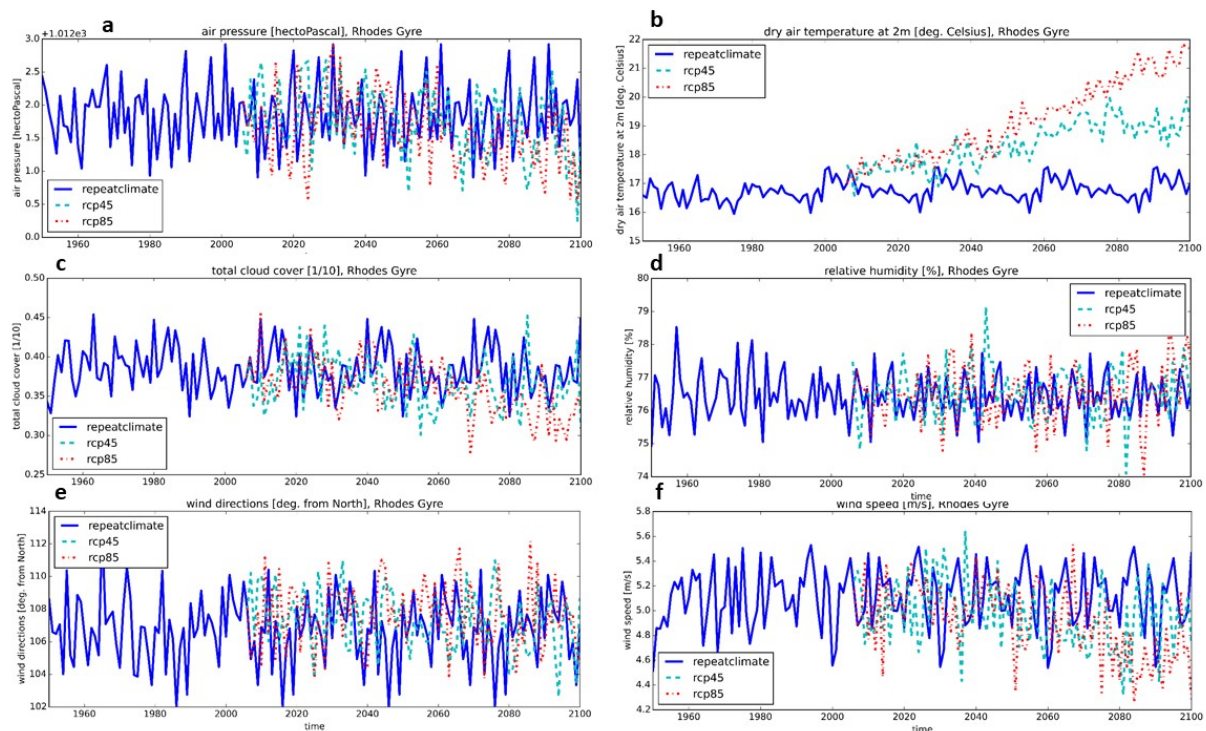


Figure S3: Future climatological conditions compared to the reference conditions (repeat of 1979-2008 climate) for the location [35.75 °N, 28.6 °E] in the Rhodes Gyre (Mediterranean): a) air pressure, b) air temperature, c) cloud cover, d) relative humidity, e) wind direction and f) wind speed.

The Rhodes Gyre area is mainly characterized by rising air temperatures (Figure S3b), from 16.5 °C to nearly 22 °C (20 °C) by the end of the 21st century under the RCP8.5 (RCP4.5) scenario

(business as usual), an increase of over 30% (20%). At the same time there is a marked decrease in wind speed, particularly for the RCP8.5 scenario, from 2050 onwards (Figure S3f).

Section S3. Comparison of CMIP5 meteorology

The applied meteorological forcing differs between the validation simulation (ECMWF ERA-Interim) and the future scenarios including the Reference simulation (CMIP5 Mediterranean downscaling product). In general, the historical temperatures are similar to the ERA-Interim ones for the winter months, but they are significantly lower in summer (more than 5 degrees). Wind velocities are similar in both meteorological models (Figure S4).

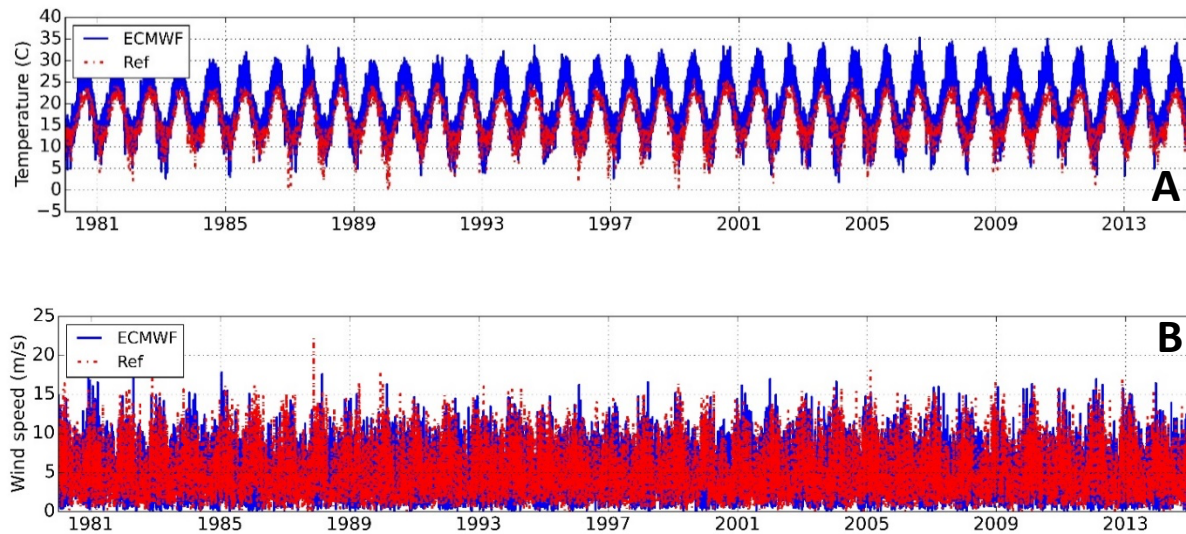


Figure S4: A) Temperatures and B) Wind speeds used to force the validation run (1980-2014), obtained from ECMWF ERA-Interim and the Reference run, obtained from the historical Med-CORDEX results.

Section S4. Model validation

Model validation was only performed for the lower trophic level model for hydrodynamics. The time evolution of the vertical profiles of temperature are shown in Figure S5 A for the validation run and B for the reference run. The validation run produces higher temperatures during the summer months, which seem to be higher than the observations. The periods of winter mixing are well reproduced in terms of temperature in both simulations, but the summer mixed layer depth is probably too deep in both cases and is not supported by any of the measured profiles.

Both models reproduce higher salinities in the first 150 m of the water column, which is in accordance with the observations (Figure S6). The differences between both simulations are minor, with the validation run giving slightly higher salinities in summer which are closer to the observations, but still underestimate them. Thus, the vertical salinity gradient is well reproduced by the model, whereas the vertical temperature gradient is too deep compared to observations. This is due to the imposed relaxation which is stronger for salinity than for temperature, in order to allow for summer warmer and winter cooling of the top mixed layer.

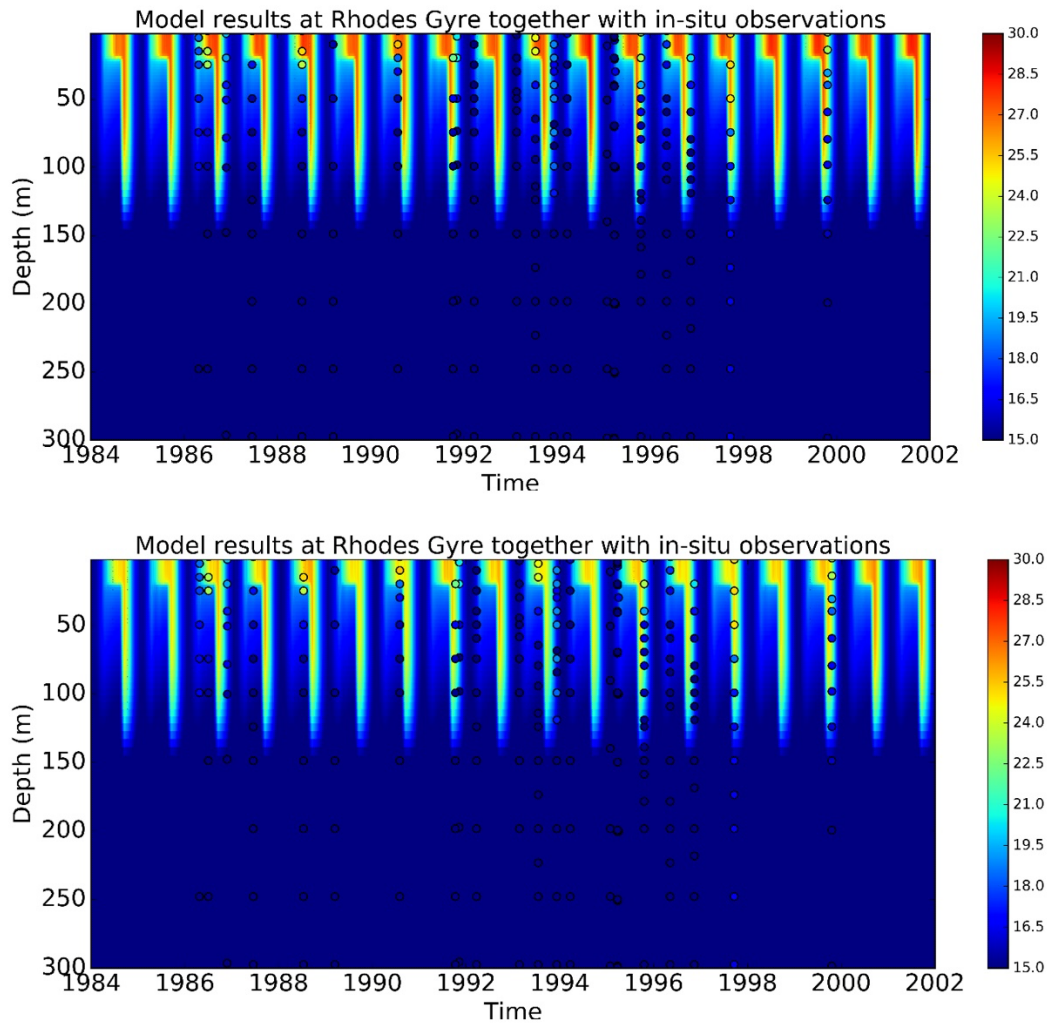


Figure S5: Vertical temperatures at the Mediterranean modelling site obtained from the results of the A) Validation run and B) Reference run, together with the available temperature observations.

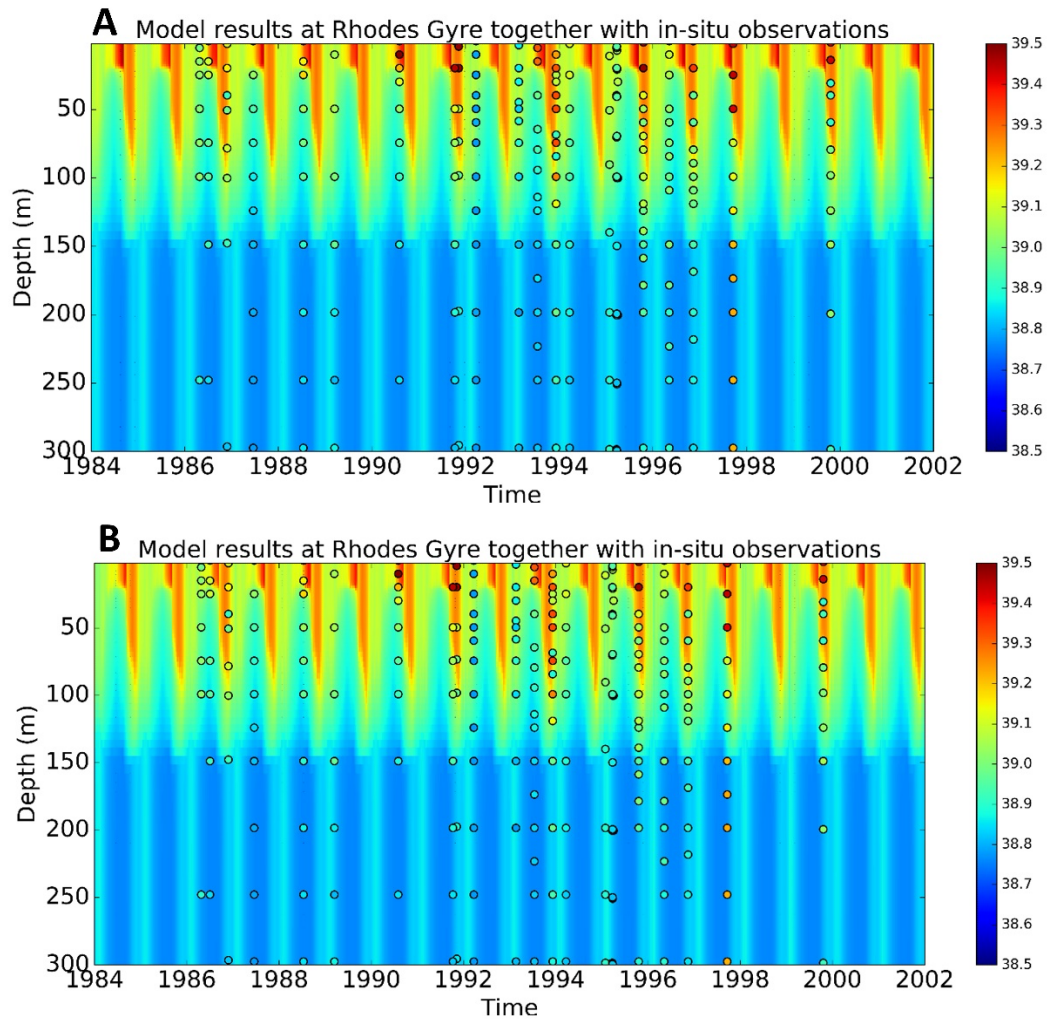


Figure S6: Vertical salinities at the Mediterranean modelling site obtained from the results of the A) Validation run and B) Reference run, together with the available salinity observations.

References

Zhang Y, Mahowald N, Scanza R, Journet E, Desboeufs K, Albani S, Kok J, Zhuang G, Chen Y, Cohen DD, Paytan A, Patey MD, Achterberg EP, Engelbrecht JP and Fomba KW (2015) Modeling the global emission, transport and deposition of trace elements associated with mineral dust. *Biogeosciences* 12:5771–5792 <https://doi.org/10.5194/bg-12-5771-2015>